

Dynamics of a single polymer chain: Ergodicity and conformation of a rotating chain

Mark P. Taylor,^{1,*} Kerem Isik,² and Jutta Luettmmer-Strathmann^{2,†}

¹*Department of Physics, Hiram College, Hiram, Ohio 44234, USA*

²*Department of Physics, University of Akron, Akron, Ohio 44325-4001, USA*

(Received 5 August 2008; published 19 November 2008)

The dynamics of an isolated polymer chain has irreversible aspects that lead to the decorrelation of configurational properties over time. For simple mechanical models with time reversible equations of motion, the irreversibility is a consequence of the chaotic nature of the dynamics which, for a many body system, is expected to result in ergodic mixing. Here we study a fixed bond length N -mer interaction-site chain with fixed total energy and angular momentum. For $N \geq 4$ the equations of motion for such a chain are nonintegrable and chaotic dynamics is expected. We directly assess the ergodicity of short repulsive Lennard-Jones chains by comparing phase space and time averages for structural and energetic properties. The phase space averages are determined from the exact microcanonical partition function while the time averages are obtained from molecular dynamics (MD) simulations. For $N=4$ and 5 we find that our exact phase space averages agree with the MD time averages, as expected for an ergodic system. The $N=3$ system is integrable and thus displays regular dynamics for which time averages are found to depend on initial conditions. In all cases, the total angular momentum is found to have a large effect on both the average chain conformation and the partitioning of the total energy between potential, vibrational, and rotational contributions. Compared to a nonrotating chain, a small to moderate angular momentum slightly speeds up the internal chain dynamics, while a large angular momentum dramatically slows the internal dynamics.

DOI: [10.1103/PhysRevE.78.051805](https://doi.org/10.1103/PhysRevE.78.051805)

PACS number(s): 36.20.Ey, 82.37.-j, 05.20.Gg, 05.45.-a

I. INTRODUCTION

Most studies of polymer chain conformation and dynamics consider polymers in solution or in the melt or solid phase [1–3]. Thus the polymer is coupled to a many-body system allowing for the exchange of thermal energy and momentum. One might expect the behavior of an *isolated* polymer chain to differ markedly from a chain in contact with a fluctuating many-body reservoir. While isolated chain molecules can be found in interstellar space [4,5], they are also routinely prepared in the laboratory in supersonic molecular beams (as for Fourier-transform microwave spectroscopy) [4] or via laser desorption or electrospray injection (as for ion mobility and mass spectrometry measurements) [6,7]. Such an isolated chain can be treated as a mechanical system for which conservation of energy, linear momentum, and angular momentum should hold. For such a fixed-energy system the microcanonical ensemble provides the natural statistical mechanical description, although the microcanonical partition function must be modified to account for momentum conservation. This type of approach has been applied to the analysis of isolated atomic clusters [8,9] and noninteracting or Gaussian chains [10,11]. In both of these cases, the average conformation and dynamics of the system as well as the partitioning of the energy between rotational and vibrational contributions is found to depend strongly on the total angular momentum.

The application of statistical mechanical methods to describe an isolated chain molecule (a few-body system) assumes that this system is ergodic (and mixing) [12]. While

actually proving a multidimensional, multiparticle system is ergodic is a notoriously difficult problem [13–15], one can at least attempt to assess ergodic-like behavior of a system via direct comparison of phase space and time averages. For an ergodic system, phase space averages obtained from the partition function will be equal to time averages (e.g., obtained by integrating the equations of motions in a molecular dynamics simulation) and these time averages will be independent of initial conditions. The ability of a many-body system to explore all accessible phase space, independent of initial starting point, typically relies on an underlying chaotic dynamics [16]. While only a small number of many-body systems have been rigorously shown to be chaotic and ergodic (such as two- and three-dimensional hard spheres in a box [13–16]), there is strong numerical evidence for chaotic dynamics (and ergodic mixing) in the numerous liquid state models studied extensively via computer simulation [17]. (However, for simulations at low energy or temperature, systems with attractive interactions tend to get trapped in local potential energy minima, and thus one must often be cautious regarding the assumption of ergodicity [18]). For spherically symmetric, *repulsive* interaction potentials, small differences in particle trajectories will be amplified in collisions (due to the convex nature of the scattering potential), providing a mechanism for chaos. Thus one might suspect that a flexible chain comprised of repulsive, spherical interaction sites would also exhibit chaotic dynamics. For chains with fixed bond length there is an additional reason to expect chaotic dynamics, even in the absence of repulsive site-site interactions, since the bond constraints themselves lead to nonlinear equations of motion [19,20].

This work begins a detailed examination of the dynamics of an isolated interaction-site polymer chain. The emphasis of this first paper is on the development of the exact microcanonical partition function for an isolated interaction site

*taylormp@hiram.edu

†jutta@uakron.edu

chain with fixed bond length. The chain is treated as a classical mechanical system subject to the conservation of total energy, linear momentum, and angular momentum. Although Deutsch has raised the issue of energy loss in such an isolated system due to the spontaneous emission of photons [10], here we will assume the time scale of this process is long enough that it can be ignored. We analytically evaluate the momentum integrals in the partition function, introducing a method to explicitly remove the momentum degrees of freedom constrained by the fixed bond length condition. We use this partition function to carry out exact calculations for configurational and energetic properties of short repulsive-sphere chains. We also carry out molecular dynamics (MD) simulations of these short chain systems and thus are able to make direct comparison between exact phase space averages and the MD time averages. Of particular interest here is the effect of total angular momentum on the conformation and energy partitioning, as well as the configurational decorrelation time of a rotating chain. In a second publication we will more fully investigate time correlation functions and the chaotic nature of the dynamics of the isolated polymer chain.

II. MODEL SYSTEM AND PHASE SPACE

The subject of this work is a single flexible chain molecule consisting of N spherically symmetric interaction sites connected by “universal joints” with fixed bond length b . The chain sites are numbered 1 through N and site i is located by the position vector \mathbf{r}_i . Nonbonded sites i and j ($|i-j| > 1$) interact via a spherically symmetric potential $u(r_{ij})$ where $r_{ij} = |\mathbf{r}_{ij}|$ and $\mathbf{r}_{ij} = \mathbf{r}_j - \mathbf{r}_i$. The bond-length constraint imposes the following restrictions on the site positions and velocities:

$$\hat{\mathbf{r}}_{i,i+1} \cdot \mathbf{r}_{i,i+1} = b, \quad i \in \{1, \dots, N-1\}, \quad (1)$$

$$\hat{\mathbf{r}}_{i,i+1} \cdot \mathbf{v}_{i,i+1} = 0, \quad (2)$$

where $\hat{\mathbf{r}}_{i,i+1}$ is the unit vector from site i to site $i+1$, $\mathbf{v}_i = d\mathbf{r}_i/dt$ is the velocity of bead i , and $\mathbf{v}_{ij} = \mathbf{v}_j - \mathbf{v}_i$.

Since we consider single chains that move freely, without external forces, the Hamiltonian for the system is the sum of kinetic and potential energy,

$$H(\{\mathbf{r}_i, \mathbf{p}_i\}) = \sum_{i=1}^N \frac{1}{2m} p_i^2 + \sum_{i=1}^{N-2} \sum_{j=i+2}^N u(r_{ij}) = K_{\text{tot}} + U(\{\mathbf{r}_i\}) = E, \quad (3)$$

where m is the bead mass, assumed to be identical for all beads, $\mathbf{p}_i = m\mathbf{v}_i$ is the momentum of bead i , and all distances and velocities satisfy the constraints given by Eqs. (1) and (2). In addition to the total energy E , both the total linear momentum $\mathbf{P}_{\text{tot}} = \sum_i \mathbf{p}_i$ and total angular momentum $\mathbf{L} = \sum_i \mathbf{r}_i \times \mathbf{p}_i$ are conserved.

The number of degrees of freedom f of a chain of N beads moving in three dimensions subject to $N-1$ bond constraints and the conservation of both linear and angular momentum is equal to

$$f = 3N - (N-1) - 6 = 2N - 5. \quad (4)$$

The phase space of the system has dimension $2f$ and, since energy is conserved, the orbits of the system are confined to a $2f-1$ dimensional subspace. For chains of three beads, the number of degrees of freedom is one and the phase-space dimension is 2. Thus the fixed energy, three-bead system is integrable and undergoes only regular motion [21,22].

For chains of four or more beads, the number of known conserved quantities is not sufficient to render the system integrable. The beads move subject to the bond constraints until they undergo collisions with nonbonded beads. Since the shape of the beads is convex, small differences between trajectories are amplified by a collision (just as in the case of the hard sphere systems [16]). Furthermore, for a purely repulsive interaction potential the system will not be trapped in potential wells at low energies. Hence we expect chaotic dynamics for chains of four or more repulsive beads. Since we have more than two degrees of freedom for these systems ($f \geq 3$ for $N \geq 4$), we expect phase space to be connected and the chaos to be global due to Arnold diffusion [22]. However, the diffusion rate for small f ($f > 2$) systems may be very slow [23,24] resulting, “for all practical purposes,” in nonergodic behavior. Also, for a chain with a very large angular momentum, only highly extended conformations will be dynamically accessible such that intrachain collisions are not possible. This may result in a crossover from chaotic to regular dynamics with increasing angular momentum.

One typically addresses the question of chaotic dynamics through an examination of Lyapunov exponents [21,22]. While such an analysis will be the subject of a future publication, here we concentrate on a comparison of phase space averages with time averages to access the ergodicity of these isolated chains.

III. ROTATING CHAIN PARTITION FUNCTION

A. Microcanonical ensemble

The microcanonical partition function for a chain of N beads at constant energy E , linear momentum \mathbf{P}_{tot} , and angular momentum \mathbf{L} can be written as

$$\begin{aligned} \omega_N(E, \mathbf{P}_{\text{tot}}, \mathbf{L}) = & \frac{1}{C} \int \delta[E - H(\{\mathbf{r}_k, \mathbf{p}_k\})] \delta^{(3)}\left(\mathbf{P}_{\text{tot}} - \sum_{i=1}^N \mathbf{p}_i\right) \\ & \times \delta^{(3)}\left(\mathbf{L} - \sum_{i=1}^N \mathbf{r}_i \times \mathbf{p}_i\right) \prod_{i=1}^{N-1} \delta(\hat{\mathbf{r}}_{i,i+1} \cdot \mathbf{r}_{i,i+1} - b) \\ & \times \delta\left(\sum_{j=1}^{N-1} (\mathbf{H}_N^{-1})_{ij} \hat{\mathbf{r}}_{j,j+1} \cdot \mathbf{p}_{j,j+1}\right) \prod_{k=1}^N d\mathbf{r}_k d\mathbf{p}_k, \quad (5) \end{aligned}$$

where C is a constant and the final product of delta functions enforce the bond length and bond velocity constraints given in Eqs. (1) and (2). The peculiar form of the bond velocity delta functions is derived in Appendix A (see also [25]). The square matrix \mathbf{H}_N , given by $\mathbf{H}_N = \mathbf{C}_N^T \mathbf{C}_N$, is the metric tensor associated with the partial coordinate transformation $\mathbf{Q}_N = \mathbf{C}_N^T \mathbf{r}$ where \mathbf{Q}_N is an $N-1$ dimensional vector of the constrained position variables $r_{i,i+1} = \hat{\mathbf{r}}_{i,i+1} \cdot \mathbf{r}_{i,i+1}$ and \mathbf{r} is a $3N$

dimensional vector with elements \mathbf{r}_i . Explicit expressions for both \mathbf{H}_N and \mathbf{C}_N are given in Appendix B.

The rotating chain partition function [Eq. (5)] is very similar to the partition function for a rotating cluster (i.e., system of nonbonded particles). In the cluster case, analytic integration over the momentum degrees of freedom is possible [8,9]. Here we follow the approach used by Calvo and Lebastie [9] for a cluster, to evaluate the chain momentum integrals (which include the bond length constraints on the velocities). Details are presented in Appendix B. For the case of $\mathbf{P}_{\text{tot}}=0$, which is equivalent to working in the chain center of mass frame, the microcanonical partition function for the N bead chain can be written as

$$\omega_N(E, \mathbf{P}_{\text{tot}}=0, \mathbf{L}) = \frac{1}{C_o} \int [E - U_L(\{\mathbf{r}_k\})]^{f/2-1} \Theta[E - U_L(\{\mathbf{r}_k\})] \times \frac{\sqrt{\det \mathbf{H}_N}^{N-1}}{\sqrt{\det \mathbf{I}_o}} \prod_{i=1}^{N-1} s(r_{i,i+1}) \prod_{k=1}^N d\mathbf{r}_k, \quad (6)$$

where U_L is an effective potential given by

$$U_L = U(\{\mathbf{r}_k\}) + \frac{1}{2} \mathbf{L}^T \mathbf{I}_o^{-1} \mathbf{L}, \quad (7)$$

$f=2N-5$ is the number of degrees of freedom, Θ is the unit step function, \mathbf{I}_o is the moment of inertia tensor with respect to the chain center of mass, $s(r)=\delta(r-b)/4\pi b^2$ is the distribution function between bonded beads [26], and the new constant is

$$C_o = \frac{\Gamma(f/2)}{\pi^{f/2}} \frac{(2N)^{3/2}}{(8\pi m b^2)^{N-1}} C. \quad (8)$$

Both the moment of inertia \mathbf{I}_o and metric tensor \mathbf{H}_N depend on the instantaneous chain configuration $\{\mathbf{r}_k\}$. The step function in Eq. (6) excludes all chain configurations for which the combination of E and \mathbf{L} is not realizable. The total energy of the system is partitioned between potential, vibrational, and rotational contributions as follows [27]:

$$E = U(\{\mathbf{r}_k\}) + K_{\text{vib}}(\{\mathbf{r}_k\}) + K_{\text{rot}}(\{\mathbf{r}_k\}), \quad (9)$$

where $K_{\text{vib}}=E-U_L$ and $K_{\text{rot}}=\frac{1}{2}\mathbf{L}^T\mathbf{I}_o^{-1}\mathbf{L}$. A nonzero value of \mathbf{L} implies a nonzero K_{rot} . Conversely, the fixed total energy E puts an upper limit on the allowed magnitude of \mathbf{L} . The exact value of this upper limit depends on the range of the site-site potential $u(r)$. If the range of the potential is less than $2b$ it is straightforward to show that this maximum possible angular momentum is $|\mathbf{L}|_{\text{max}}=\sqrt{N(N^2-1)mb^2E/6}$ (corresponding to a linear chain rotating about a principle axis with the maximum moment of inertia).

B. Temperature and the canonical ensemble

We can make the connection between the above microcanonical formalism and the more usual temperature dependent canonical representation by constructing the canonical partition function $Q_N(T, \mathbf{P}_{\text{tot}}, \mathbf{L})$ which is related to $\omega_N(E, \mathbf{P}_{\text{tot}}, \mathbf{L})$ via a Laplace transform on the energy (cf. [9,28]). Performing the Laplace transform of Eq. (6) we find

$$Q_N(T, \mathbf{P}_{\text{tot}}=0, \mathbf{L}) = \frac{1}{C_o} \frac{\Gamma(f/2)}{\beta^{f/2}} \times \int e^{-\beta U_L} \frac{\sqrt{\det \mathbf{H}_N}^{N-1}}{\sqrt{\det \mathbf{I}_o}} \prod_{i=1}^{N-1} s(r_{i,i+1}) \prod_{k=1}^N d\mathbf{r}_k, \quad (10)$$

where $\beta=1/(k_B T)$. The average total energy at a given temperature is given by

$$\langle E \rangle_T = - \frac{\partial \ln(Q_N)}{\partial \beta} = \frac{f}{2} k_B T + \langle U_L \rangle_T, \quad (11)$$

where $\langle \dots \rangle_T$ indicates the average in the canonical ensemble. Noting that $\langle E \rangle_T = \langle K_{\text{vib}} \rangle_T + \langle U_L \rangle_T$ we can define the temperature through the relation

$$k_B T = \frac{2}{f} \langle K_{\text{vib}} \rangle_T \approx \frac{2}{f} \langle K_{\text{vib}} \rangle_E. \quad (12)$$

Of course we can define temperature directly from the microcanonical partition function through the definition $1/T = (\partial S / \partial E)_{N,V}$ where the entropy is given by $S = k_B \ln \omega(E)$. However, the result of this calculation only agrees with Eq. (12) to order $1/N$ and thus care must be taken in defining thermodynamic functions for small N systems [28,29]. We have in fact confirmed that Eq. (12) provides a consistent definition of temperature for short chains by comparing exact phase space averages computed in both the microcanonical and canonical ensembles. Equation (12) can be obtained directly from the microcanonical formalism using the alternate definition of this ensemble in which one integrates over all energy states less than or equal to E rather than just those states in a shell near E as is done in Eq. (5) [28,29].

IV. CHAIN CONFORMATION AND PHASE-SPACE AVERAGES

A. Site-site probability functions

Equation (6) gives the microcanonical partition function as a weighted integral over all chain conformations. The probability density to find the chain in a specific conformation $\{\mathbf{r}_1, \dots, \mathbf{r}_N\}$ is thus given by

$$P^{(N)}(\mathbf{r}_1, \dots, \mathbf{r}_N; E, \mathbf{L}) = \frac{1}{C_o \omega_N(E, \mathbf{L}) V} [E - U_L(\{\mathbf{r}_k\})]^{f/2-1} \times \Theta[E - U_L(\{\mathbf{r}_k\})] \times \frac{\sqrt{\det \mathbf{H}_N}^{N-1}}{\sqrt{\det \mathbf{I}_o}} \prod_{i=1}^{N-1} s(r_{i,i+1}), \quad (13)$$

where V is the system volume and here and in the following we suppress the argument $\mathbf{P}_{\text{tot}}=0$. The analogous canonical probability density can be similarly obtained from Eq. (10). The N -site probability density allows one to construct the phase-space average of any configuration dependent quantity A as follows:

$$\langle A(E, \mathbf{L}) \rangle = \int A(\mathbf{r}_1, \dots, \mathbf{r}_N; E, \mathbf{L}) P^{(N)}(\mathbf{r}_1, \dots, \mathbf{r}_N; E, \mathbf{L}) \prod_{k=1}^N d\mathbf{r}_k. \quad (14)$$

Thus, for example, one can compute the phase-space average of Eq. (9) to determine the equilibrium partitioning of the total energy E between the contributions $\langle U(E, \mathbf{L}) \rangle$, $\langle K_{\text{vib}}(E, \mathbf{L}) \rangle$, and $\langle K_{\text{rot}}(E, \mathbf{L}) \rangle$. Similarly, one can compute average chain size in terms of mean-square site-site distances $\langle r_{ij}^2 \rangle$ or radius of gyration $\langle R_g^2 \rangle = \frac{1}{N^2} \sum_{i < j}^N \langle r_{ij}^2 \rangle$.

In terms of structural properties, the above N -site probability density provides a complete description of chain conformation, however, in general this full N -body function is not practical to compute. A more manageable description of the conformation of a rotating chain is provided by reduced versions of the full N -site function, such as the two-site function

$$P_{ij}^{(2)}(\mathbf{r}_i, \mathbf{r}_j; E, \mathbf{L}) = \int P^{(N)}(\mathbf{r}_1, \dots, \mathbf{r}_N; E, \mathbf{L}) \prod_{k \neq i, j}^N d\mathbf{r}_k \quad (15)$$

or the angle averaged version

$$P_{ij}(r_{ij}; E, |\mathbf{L}|) = r_{ij}^2 V \int \left(\int_0^{2\pi} d\varphi_{ij} \int_0^\pi d\theta_{ij} \sin \theta_{ij} \right. \\ \left. \times P^{(N)}(\mathbf{r}_1, \dots, \mathbf{r}_N; E, \mathbf{L}) \right) \prod_{k \neq i, j}^N d\mathbf{r}_{ik}. \quad (16)$$

In Eq. (16) the angles θ_{ij} and φ_{ij} specify the orientation of the vector \mathbf{r}_{ij} with respect to \mathbf{L} and the angular average is carried out over a fixed chain conformation $\{\mathbf{r}_{i1}, \dots, \mathbf{r}_{iN}\}$ about the chain center of mass. Note that while the Eq. (13) and (15) probability functions depend on the orientation of the angular momentum \mathbf{L} , the angle averaged two-site function [Eq. (16)] only depends on the magnitude $|\mathbf{L}|$. For $\mathbf{L} = 0$, the N -site probability function $P^{(N)}(\mathbf{r}_1, \dots, \mathbf{r}_N; E, 0)$ is independent of the orientation of \mathbf{r}_{ij} so Eq. (16) simplifies to

$$P_{ij}(r_{ij}; E, 0) = 4\pi r_{ij}^2 V \int P^{(N)}(\mathbf{r}_1, \dots, \mathbf{r}_N; E, 0) \prod_{k \neq i, j}^N d\mathbf{r}_{ik}. \quad (17)$$

B. Exact expressions for short chains

The above two-site functions can be computed exactly for short chains following the approach of Refs. [26,30]. For these exact calculations it is convenient to work in a “body” coordinate system with a chain site, rather than the center of mass, at the origin. These body coordinates are constructed in terms of three reference sites, α , β , and γ , that define the body coordinate z axis and xz plane as follows: $\mathbf{x}_\alpha^T = [0, 0, 0]$, $\mathbf{x}_\beta^T = [0, 0, r_{\alpha\beta}]$, $\mathbf{x}_\gamma^T = [r_{\alpha\gamma} \sin \theta_\gamma, 0, r_{\alpha\gamma} \cos \theta_\gamma]$. All other sites are located by body coordinates $\mathbf{x}_\delta^T = [r_{\alpha\delta} \sin \theta_\delta \cos \phi_\delta, r_{\alpha\delta} \sin \theta_\delta \sin \phi_\delta, r_{\alpha\delta} \cos \theta_\delta]$. The components of the chain moment of inertia tensor with respect to reference site α are given by

$$J_{i,j} = m \sum_{k=1}^N (\mathbf{x}_k^T \mathbf{x}_k \delta_{ij} - x_k^{(i)} x_k^{(j)}) \quad (18)$$

and the required inertia tensor with respect to the chain center of mass, $\mathbf{R}_{cm} = \frac{1}{N} \sum_{k=1}^N \mathbf{x}_k$, can be constructed using the generalized parallel axis theorem [21] as follows:

$$(\mathbf{I}_o)_{i,j} = J_{i,j} - Nm(\mathbf{R}_{cm}^T \mathbf{R}_{cm} \delta_{ij} - R_{cm}^{(i)} R_{cm}^{(j)}). \quad (19)$$

We note that the chain radius of gyration can be expressed in terms of the eigenvalues λ_i of \mathbf{I}_o as $R_g^2 = (\lambda_1 + \lambda_2 + \lambda_3) / 2Nm = \text{Tr}(\mathbf{I}_o) / 2Nm$, where Tr denotes the trace of a matrix.

In the following we refer to the “body frame” of the chain as the above defined body coordinate system with origin shifted to the chain center of mass. For $\mathbf{L} \neq 0$ this body frame will rotate with respect to a fixed space coordinate system such that the chain angular momentum within the body frame can be written as

$$\mathbf{L} = \begin{pmatrix} |\mathbf{L}| \sin \theta \cos \varphi \\ |\mathbf{L}| \sin \theta \sin \varphi \\ |\mathbf{L}| \cos \theta \end{pmatrix}, \quad (20)$$

where θ and φ give the instantaneous orientation of \mathbf{L} with respect to the body-frame axes. For an ergodic system, \mathbf{L} within the body frame will sweep through all dynamically accessible orientations and dynamical time averages will be averaged over the body-frame orientations of \mathbf{L} . Thus, for example, dynamical averages for the site-site probability functions will be identical to the orientationally averaged $P_{ij}(r; E, |\mathbf{L}|)$ given by Eq. (16). To construct exact explicit expressions for $P_{ij}(r; E, |\mathbf{L}|)$ it is useful to write this probability function in the form

$$P_{ij}(r; E, |\mathbf{L}|) = \frac{r^2 D_{ij}^{(N)}(r; E, |\mathbf{L}|)}{\int_0^{|i-j|b} r^2 D_{ij}^{(N)}(r; E, |\mathbf{L}|) dr}, \quad (21)$$

where

$$D_{ij}^{(N)}(r_{ij}; E, |\mathbf{L}|) = \int W_N \left(\frac{\det \mathbf{H}_N}{\det \mathbf{I}_o} \right)^{1/2} F_N(r_{ij}, \mathbf{X}_N; E, |\mathbf{L}|) d\mathbf{X}_N \quad (22)$$

with the orientational average given by

$$F_N(r_{ij}, \mathbf{X}_N; E, |\mathbf{L}|) = \int_0^{2\pi} d\varphi \int_0^\pi d\theta \sin \theta [E - U_L(r_{ij}, \mathbf{X}_N)]^{N-7/2} \\ \times \Theta[E - U_L(r_{ij}, \mathbf{X}_N)]. \quad (23)$$

In the above expression for the $D_{ij}^{(N)}$ functions the $N-1$ bond length constraint integrations have been carried out, resulting in the weight factor $W_N(r_{ij}, \mathbf{X}_N)$, and the instantaneous configuration of the chain is expressed using the set of $2N-5$ internal coordinates $\{r_{ij}, \mathbf{X}_N\}$ [30].

I. $N=3$

For the case of $N=3$ the single variable r_{13} completely specifies the internal conformation of the chain. We define

the body frame through reference sites $(\alpha, \beta, \gamma) = (1, 3, 2)$ and the required angle θ_2 is given by $\cos \theta_2 = r_{13}/2b$. The moment of inertia tensor \mathbf{I}_o is diagonal in this body frame with components $I_{xx} = mr_{13}^2/2$, $I_{yy} = m(2b^2 + r_{13}^2)/3$, $I_{zz} = m(4b^2 - r_{13}^2)/6$ and the conformation dependent rotational kinetic energy is given by

$$K_{rot}(r_{13}, \mathbf{L}) = \frac{1}{2} \mathbf{L}^T \mathbf{I}_o^{-1} \mathbf{L} = \frac{L_x^2}{2I_{xx}} + \frac{L_y^2}{2I_{yy}} + \frac{L_z^2}{2I_{zz}}, \quad (24)$$

where the L_α are the body-frame Cartesian components of $\mathbf{L}(\theta, \varphi)$ as given in Eq. (20). As noted above, the $N=3$ system is integrable and in Appendix C we give equations of motion for the chain end-to-end distance and the body-frame orientation of the \mathbf{L} vector. The motion of the 3-mer chain is similar to that of an asymmetric rigid body, in that for \mathbf{L} initially parallel to one of the body-frame axes (which are principle axes), the orientation of \mathbf{L} remains fixed in the body frame. In this case the end-to-end probability function for the chain is simply obtained from the $r_{13}(t)$ equation of motion, being given by $P_{13}^{(3)}(r; E, \mathbf{L}) = A/\dot{r}_{13}$ where A is a normalization constant and $\dot{r}_{13} = dr_{13}/dt$ is given by Eq. (C1). The phase space version of this probability function is given by the nonangle averaged version of Eq. (21) with the following \mathbf{L} -dependent D function

$$D_{13}^{(3)}(r_{13}; E, \mathbf{L}) = \frac{1}{8\pi b^2 r_{13}} \left(\frac{\det \mathbf{H}_3}{\det \mathbf{I}_o} \right)^{1/2} \times \frac{\Theta[E - u(r_{13}) - K_{rot}(r_{13}, \mathbf{L})]}{\sqrt{E - u(r_{13}) - K_{rot}(r_{13}, \mathbf{L})}}, \quad (25)$$

where $\det \mathbf{H}_3 = 4 - (\hat{\mathbf{r}}_{12} \cdot \hat{\mathbf{r}}_{23})^2 = 4 - (1 - r_{13}^2/2b^2)^2$ and $\det \mathbf{I}_o = I_{xx} I_{yy} I_{zz}$. Comparison of Eqs. (25) and (C1) show that for principle axis rotation, the phase space and dynamical versions of $P_{13}^{(3)}(r; E, \mathbf{L})$ are identical and thus phase space and time averages for configurational properties will be the same. We note that these properties depend on the rotation axis as $P_{13}^{(3)}(r; E, L\hat{\mathbf{x}}) \neq P_{13}^{(3)}(r; E, L\hat{\mathbf{y}}) \neq P_{13}^{(3)}(r; E, L\hat{\mathbf{z}})$. When \mathbf{L} is not initially aligned along a body-frame axis, $\mathbf{L}(\theta, \varphi)$ will trace a path within the body frame and the above D function would have to be averaged over this path to obtain a site-site probability function that reproduces dynamical time averages. Even for this more general motion, we anticipate that dynamical averages will not cover the entire configurational phase space and will, in general, depend on the initial orientation of \mathbf{L} . For the case of $\mathbf{L}=0$, there is no coupling between orientation and energy and thus dynamical averages for configurational properties are identical to the phase space results given by Eq. (21) with

$$D_{13}^{(3)}(r_{13}; E, 0) = \frac{1}{2b^2 r_{13}} \left(\frac{\det \mathbf{H}_3}{\det \mathbf{I}_o} \right)^{1/2} \frac{\Theta[E - u(r_{13})]}{\sqrt{E - u(r_{13})}}. \quad (26)$$

2. $N=4$

For the case of $N=4$ we define the body frame through reference sites $(\alpha, \beta, \gamma) = (1, 3, 4)$ and use the set of variables $\{r_{14}, r_{13}, \phi_2\}$ to specify the internal chain conformation. Explicit location of sites 2 and 4 in the body frame requires the

angles θ_2 and θ_4 , which are given by $\cos \theta_2 = r_{13}/2b$ and $\cos \theta_4 = (r_{13}^2 + r_{14}^2 - b^2)/2r_{13}r_{14}$, respectively. The $N=4$ system is expected to display chaotic dynamics and, assuming ergodicity, dynamical averages should cover the entire configurational phase space and be independent of the initial orientation of \mathbf{L} . The angle averaged D functions required for the two 4-mer site-site probability function can be written as

$$D_{13}^{(4)}(r_{13}; E, |\mathbf{L}|) = \frac{1}{16\pi^2 b^3 r_{13}^2} \int_{|r_{13}-L|}^{r_{13}+L} dr_{14} r_{14} \int_0^\pi d\phi_2 \times \left(\frac{\det \mathbf{H}_4}{\det \mathbf{I}_o} \right)^{1/2} F_4(r_{14}, r_{13}, \phi_2; E, |\mathbf{L}|) \quad (27)$$

and

$$D_{14}^{(4)}(r_{14}; E, |\mathbf{L}|) = \frac{1}{16\pi^2 b^3 r_{14}^2} \int_{|r_{14}-L|}^{\min(2L, r_{14}+L)} dr_{13} \int_0^\pi d\phi_2 \times \left(\frac{\det \mathbf{H}_4}{\det \mathbf{I}_o} \right)^{1/2} F_4(r_{14}, r_{13}, \phi_2; E, |\mathbf{L}|), \quad (28)$$

where $\det \mathbf{H}_4 = 2 \det \mathbf{H}_3 - 2(\hat{\mathbf{r}}_{23} \cdot \hat{\mathbf{r}}_{34})^2$.

3. $N=5$

For the case of $N=5$ we define the body frame through reference sites $(\alpha, \beta, \gamma) = (3, 1, 5)$ and use the set of variables $\{r_{15}, r_{13}, r_{35}, \psi_4, \phi_2\}$ to specify the internal chain conformation. Explicit location of chain sites 2, 4, and 5 in the body frame requires the angles θ_2 , θ_4 , θ_5 , and ϕ_4 . The needed polar angles are given by $\cos \theta_2 = r_{13}/2b$, $\cos \theta_4 = \cos \theta_5 \cos \gamma_{45} + \sin \theta_5 \sin \gamma_{45} \cos \psi_4$, and $\cos \theta_5 = (r_{13}^2 + r_{35}^2 - r_{15}^2)/2r_{13}r_{35}$, where $\cos \gamma_{45} = r_{35}/2b$, and the azimuthal angle ϕ_4 is defined via $\cos \gamma_{45} = \cos \theta_4 \cos \theta_5 + \sin \theta_4 \sin \theta_5 \cos \phi_4$. The $N=5$ system is expected to display chaotic dynamics and, assuming ergodicity, dynamical averages should cover the entire configurational phase space and be independent of the initial orientation of \mathbf{L} . The angle averaged D function required for the 5-mer end-to-end probability function can be written as

$$D_{15}^{(5)}(r_{15}; E, |\mathbf{L}|) = \frac{1}{64\pi^3 b^4 r_{15}} \int_{\max(0, r_{15}-2L)}^{2L} dr_{13} \times \int_{|r_{15}-r_{13}|}^{\min(2L, r_{15}+r_{13})} dr_{35} \int_0^\pi d\psi_4 \int_0^{2\pi} d\phi_2 \times \left(\frac{\det \mathbf{H}_5}{\det \mathbf{I}_o} \right)^{1/2} F_5(r_{15}, r_{13}, r_{35}, \psi_4, \phi_2; E, |\mathbf{L}|), \quad (29)$$

where $\det \mathbf{H}_5 = 2 \det \mathbf{H}_4 - (\hat{\mathbf{r}}_{34} \cdot \hat{\mathbf{r}}_{45})^2 \det \mathbf{H}_3$. Expressions for the D functions associated with the other 5-mer site-site probability functions can be constructed by appropriate generalization of Eqs. (20)–(24) in Ref. [26].

V. RESULTS FOR SOFT-SPHERE CHAINS

The results developed in the preceding section are valid for a flexible chain for which the site-site potential energy function $u(r)$ is spherically symmetric. In the following we will specialize to a repulsive soft-sphere, or truncated-shifted Lennard-Jones, potential given by

$$u(r) = \begin{cases} 4\epsilon \left[\left(\frac{\sigma}{r} \right)^{12} - \left(\frac{\sigma}{r} \right)^6 \right] + \epsilon, & r < r_c \\ 0, & r \geq r_c \end{cases}, \quad (30)$$

where $r_c = 2^{1/6}\sigma$. The potential energy, as well as the corresponding force, $f(r) = -\nabla u(r)$, vanish continuously as the distance r between beads approaches the cut off distance r_c . For our model chain we fix the bond length to be $b = \sigma$. The potential parameters ϵ and σ set the energy and distance scales, respectively, and allow us to define a dimensionless angular momentum $L^* = L/\sigma(m\epsilon)^{1/2}$. For this model chain, the maximum angular momentum possible for a chain with total energy E is $L_{\max}^* = \sqrt{\frac{1}{6}N(N^2-1)E/\epsilon}$.

A. Simulation methods and time averages

We have carried out molecular dynamics simulations of the isolated soft-sphere chain using both the SHAKE and RATTLE algorithms [31–34]. These methods enforce the fixed bond length and velocity constraints of Eqs. (1) and (2) using an iterative procedure. To prevent bond crossing, a potential of 900ϵ is associated with a chain conformation that allows two bonds to cross each other. Energies in the work presented here are well below this threshold so that bond-crossing is prohibited and thus we are modeling truly self-excluding, as opposed to “phantom,” chains.

For these simulations the initial configuration of the N -bead chain is generated at random, subject to the Eq. (1) constraint, and random velocities are assigned to each bead. Relative velocity components along the bonds are removed to satisfy Eq. (2) and tangential velocity components are removed to give $L=0$. The rotational kinetic energy $K_{rot} = \frac{1}{2}\mathbf{L}^T\mathbf{I}_o^{-1}\mathbf{L}$ and potential energy U are computed for this chain configuration and velocities are rescaled to yield the required value of $K_{vib} = E - U - K_{rot}$. Finally, tangential velocities are added to produce the desired \mathbf{L} . The simulation uses the Verlet algorithm with a time step of $\Delta t = 5 \times 10^{-4}$ where time t is measured in units of $\sigma(m/\epsilon)^{1/2}$. Simulations are run for $10^8 - 10^9$ time steps over which the energy remains constant to better than 0.01% and variations in the angular momentum are significantly smaller than 0.01%. Uncertainty estimates in equilibrium properties are obtained via block averaging.

In an MD simulation we can construct time averages of any configuration dependent property A via

$$\langle A(E, \mathbf{L}) \rangle_{\text{time}} = \frac{1}{\tau_{\text{run}}} \int_0^{\tau_{\text{run}}} A(\mathbf{r}_1(t), \dots, \mathbf{r}_N(t); E, \mathbf{L}) dt, \quad (31)$$

where τ_{run} is the total simulation time. For an ergodic system, this time average will equal the phase space average defined in Eq. (14). We can similarly construct the time autocorrelation function for A as follows:

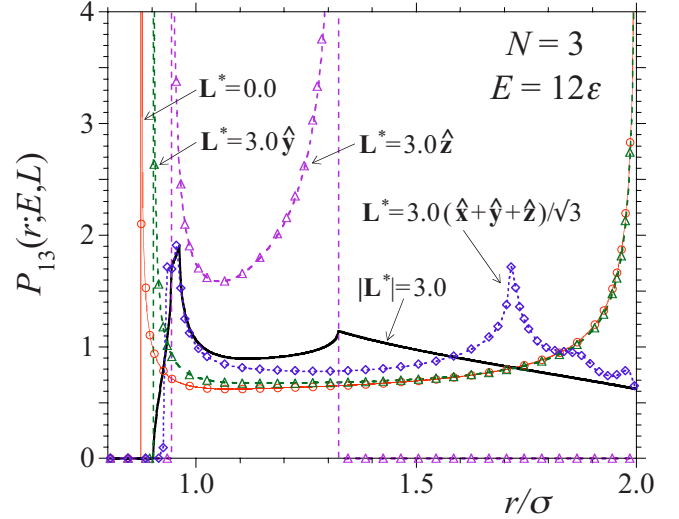


FIG. 1. (Color online) End-to-end probability function $P_{13}(r; E, L)$ for an $N=3$ chain with total energy $E=12\epsilon$ and reduced angular momentum $L^*=0$ and 3. The symbols are results from MD simulations using different initial \mathbf{L} vectors as indicated. The solid and dashed lines are results from the angle-averaged $P_{13}(r; E, |L|)$ and angle-dependent $P_{13}(r; E, \mathbf{L})$ phase-space probability densities, respectively. The dotted line, shown for the case of a nonprinciple initial rotation axis, has been obtained via numerical solution of the Appendix C equations of motion with the same initial conditions of $r_{13}(0) = 1.4b$ and $\dot{r}_{13}(0) < 0$ as used in the corresponding MD simulation.

$$\langle A(0)A(t) \rangle = \frac{1}{\tau_c} \int_0^{\tau_c} dt' A(t')A(t'+t), \quad (32)$$

where $t < \tau_c < \tau_{\text{run}}$. For an ergodic mixing system this type of configurational correlation function will decay in time, approaching the phase space average $\langle A \rangle^2$ in the limit of $t \rightarrow \infty$ [35].

B. Comparison of exact phase space and MD time averages

In this work our results are limited to very short chains ($N \leq 5$) to allow for direct comparison between exact phase space averages (detailed in Sec. IV) and the time averages obtained from the MD simulations. The integrals required for the phase space averages were computed numerically using Gaussian-Legendre quadrature. The lower integration limits for these integrals were set using the energy Θ function in the integrand.

In Fig. 1 we show the end-to-end probability function for an $N=3$ chain with total energy $E=12\epsilon$ and total angular momentum $L^*=0$ and 3 (noting that $L_{\max}^* = \sqrt{48} \approx 6.9$) obtained from MD simulation (symbols) and phase-space averages (solid and dashed lines). For the nonrotating chain ($L^*=0$) the MD results, which are time averages, agree with the phase-space results obtained using Eq. (26). The shape of the probability function is characteristic of regular oscillatory motion where the lower turning point is set by the condition $u(r_{\min}) = E$ and the upper turning point is set by the bond constraint $r_{\max} = 2b$. For the rotating chain ($L^*=3$) results are

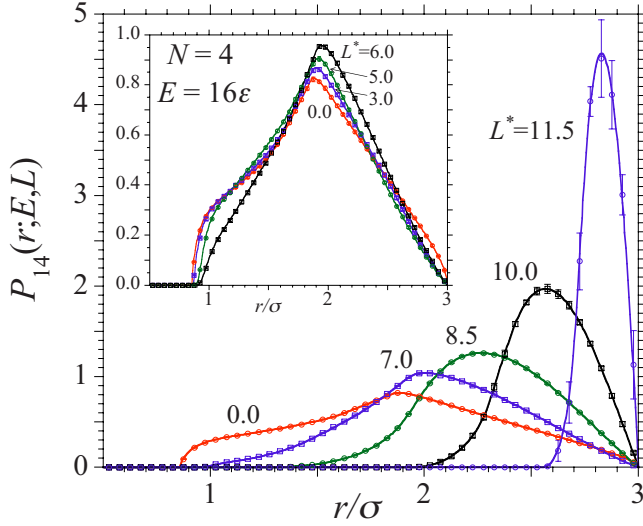


FIG. 2. (Color online) End-to-end probability function $P_{14}(r; E, L)$ for an $N=4$ chain with total energy $E=16\epsilon$ and reduced angular momentum L^* as indicated. The solid lines are results from the exact phase-space averages given by Eqs. (21) and (28) while the symbols are time average results obtained from MD simulations. The latter results are found to be independent of the orientation of the initial (dynamically allowed) \mathbf{L} vector.

shown for three different initial \mathbf{L} vectors, two corresponding to principle axis rotation (\hat{y} and \hat{z}) and one for initial rotation about a nonprinciple axis ($\hat{x} + \hat{y} + \hat{z}$). For principle axis rotation the MD results are independent of the initial r_{13} value and agree with the non-angle-averaged phase-space results computed using Eq. (25). For nonprinciple axis rotation the end-to-end probability function depends on the initial \mathbf{L} vector as well as the initial value of r_{13} and the initial sign of \dot{r}_{13} . For an ergodic-mixing system this probability function would be independent of initial conditions and be equal to the angle-averaged phase-space result shown in Fig. 1 as the solid bold line. Clearly the $N=3$ chain is a nonergodic, non-mixing system. Although not shown here, we note that for increasing angular momentum the minimum allowed r_{13} distance increases such that above some critical L^* value $P_{13}(r)=0$ for $r < r_c$. In this large angular momentum regime there are no bead-bead collisions and the dynamics is driven by “collisions” between the end beads and the centrifugal barrier. The upper cutoff in the Fig. 1 probability function for $\mathbf{L}=L\hat{z}$ is similarly due to such collisions.

In Figs. 2–5 we show conformation and energy partitioning results for rotating $N=4$ and 5 chains with total energy $E=4N\epsilon$ for a range of angular momenta. The maximum angular momentum for the $N=4$ and 5 chains are $L^*_{\max}=12.6$ and 20, respectively. The site-site probability functions shown in Figs. 2 and 3 and the average chain dimensions shown in Fig. 4 demonstrate that the chain conformation becomes increasingly extended with increasing angular momentum. As for the $N=3$ chain, for large L^* the probability for bead-bead collisions is essentially zero as $P_{ij}(r) \approx 0$ for $r < r_c$. This conclusion is confirmed by the energy results presented in Fig. 5 where the average total potential energy $\langle U \rangle$ goes to zero for large L^* . With increasing L^* the chain experiences a monotonic increase in rotational kinetic energy

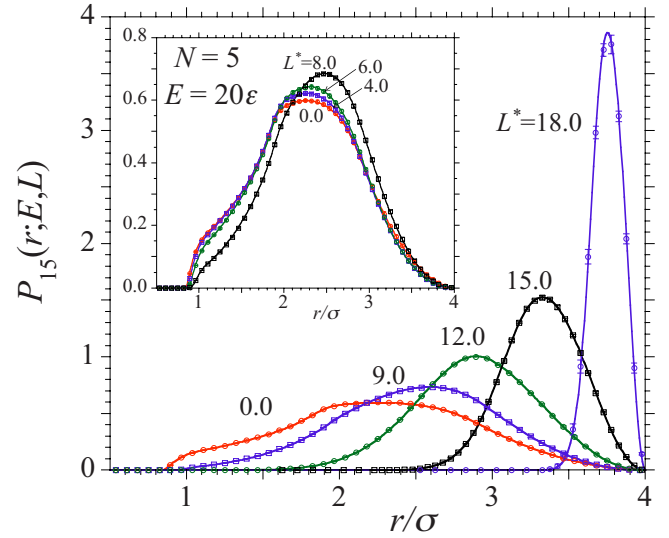


FIG. 3. (Color online) End-to-end probability function $P_{15}(r; E, L)$ for an $N=5$ chain with total energy $E=20\epsilon$ and reduced angular momentum L^* as indicated. The solid lines are results from the exact phase space averages given by Eqs. (21) and (29) while the symbols are time average results obtained from MD simulations. The latter results are found to be independent of the orientation of the initial (dynamically allowed) \mathbf{L} vector.

at the expense of potential and vibrational kinetic energy. Since the temperature of the system is proportional to the vibrational kinetic energy [see Eq. (12)], Fig. 5 shows that, for fixed total energy, increasing angular momentum reduces the chain temperature.

We expect the rate at which the chain is able to explore configuration space depends on the bead collision rate. With

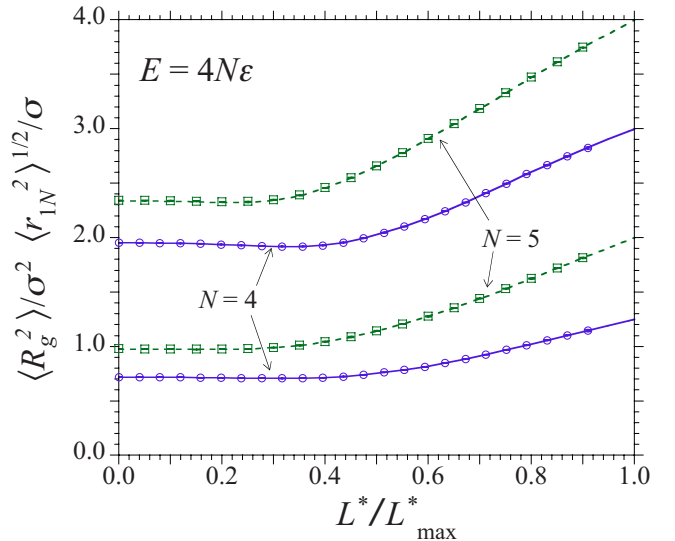


FIG. 4. (Color online) Mean square radius of gyration $\langle R_g^2 \rangle$ (lower curves) and root-mean-square end-to-end distance $\langle r_{1N}^2 \rangle^{1/2}$ (upper curves) for $N=4$ and 5 chains with total energy $E=4N\epsilon$ vs scaled reduced angular momentum L^*/L^*_{\max} . The solid and dashed lines are results from the exact phase space averages given by Eq. (14) while the symbols are time average results obtained from MD simulations. The latter results are found to be independent of the orientation of the initial (dynamically allowed) \mathbf{L} vector.

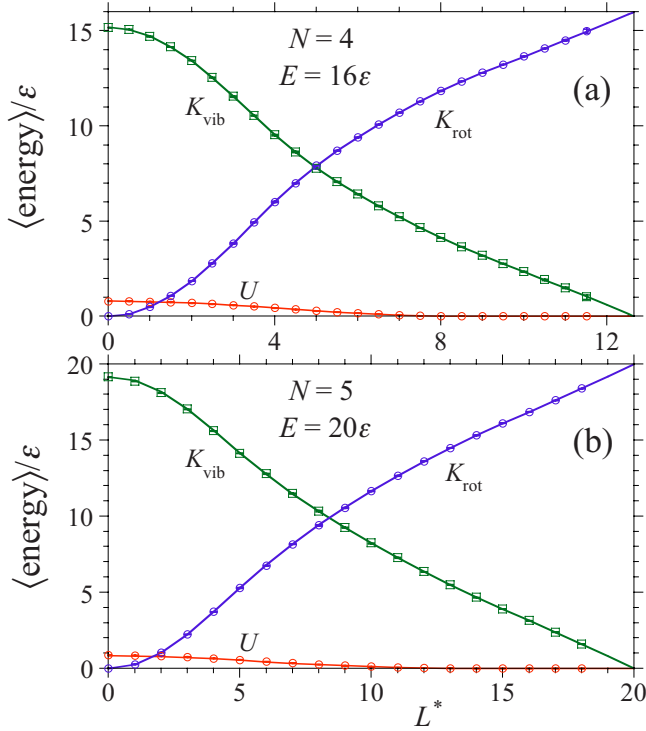


FIG. 5. (Color online) Average potential, vibrational, and rotational energies, as indicated, for (a) an $N=4$ and (b) an $N=5$ chain with total energy $E=4N\epsilon$ vs reduced angular momentum L^* . The solid lines are results from the exact phase-space averages given by Eq. (14) while the symbols are time average results obtained from MD simulations. The latter results are found to be independent of the orientation of the initial (dynamically allowed) \mathbf{L} vector.

less energy available for bead-bead or bead-centrifugal barrier collisions we expect slower dynamics for a more rapidly rotating chain. However, the near perfect agreement between our exact phase-space averages and the MD time averages, even for very large angular momentum, strongly suggests that these rotating chain systems are indeed ergodic over the full range of angular momentum. Of course the volume of accessible phase space decreases with increasing L^* such that in the limit of $L^* \rightarrow L_{\text{max}}^*$ the dynamics are restricted to regular rotation of a linear chain about a perpendicular axis. The question of crossover from chaotic to regular dynamics with increasing L^* awaits a full investigation of the Lyapunov exponents of this system.

C. Configurational decorrelation time

For an ergodic mixing system we expect correlations of time dependent configurational properties, as defined by Eq. (32), to decay in time. For chain molecules, the end-to-end vector is one such configurational property with correlations described by the function

$$C(t) = \langle \mathbf{r}_{1N}(0) \cdot \mathbf{r}_{1N}(t) \rangle. \quad (33)$$

In Fig. 6 we show this end-to-end vector correlation function $C(t)$ for both nonrotating ($L^*=0$) and rotating ($L^* \neq 0$) $N=4$ and $N=5$ chains. In all cases the function exhibits an

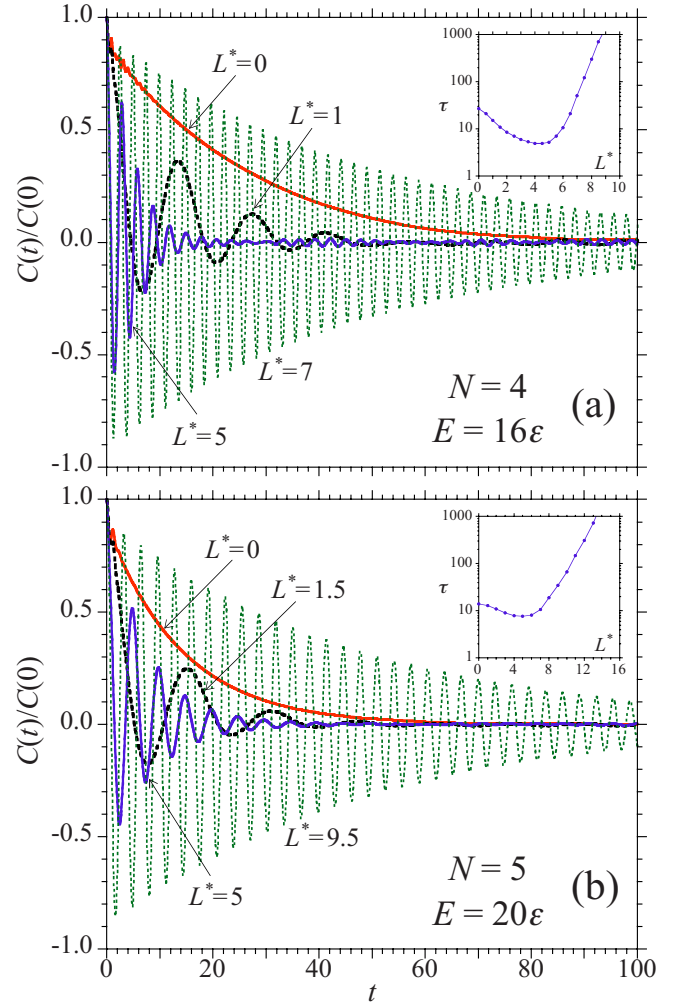


FIG. 6. (Color online) Chain end-to-end vector time correlation function $C(t)/C(0)$ for (a) an $N=4$ and (b) an $N=5$ chain with total energy $E=4N\epsilon$ and reduced angular momentum of L^* , as indicated, versus time t . All results shown are obtained from MD simulation. The nonrotating chains ($L^*=0$) exhibit a smooth and nearly monotonic decay in this correlation function while the results for the rotating chains ($L^* \neq 0$) display strong oscillations. Slow rotation (small L^*) causes a faster decay of the correlations compared to the nonrotating chain while fast rotation (large L^*) results in a slower decay. Inset: Exponential decay time τ vs reduced angular momentum L^* .

initial rapid drop followed by a slower exponential-like decay approximately described by $C(t)/C(0) \approx A \cos(\omega t) \times \exp(-t/\tau)$. For the nonrotating chain the decay of correlations is monotonic (i.e., $\omega=0$) while for the rotating chain this decay is oscillatory with the frequency of oscillation increasing monotonically with angular momentum (i.e., $\omega \sim L^*$). Interestingly, the decay time τ vs angular momentum is nonmonotonic, decreasing for slow rotation and then rapidly increasing for sufficiently fast rotation. This speed up in the dynamics for a slowly rotating chain is surprising since the effect of rotation is to lower the effective temperature [given by Eq. (12)] of the chain. While the speed up of the end-to-end vector decorrelation for the slowly rotating chain is certainly coupled to the increase in phase-space volume

sampled, there may also be a contribution to this speedup due to an increased number of collision events (which now include collisions between beads and the centrifugal barrier). In the case of rapidly rotating chains, as discussed above, direct bead-bead collisions are no longer possible and the dynamics is controlled by bead-barrier collisions only. This reduction in the number of collision events, along with the dynamically restricted range of directions for the end-to-end vector, lead to the very slow decay in correlations for the large angular momentum chain. In the limit of $L^* \rightarrow L_{\max}^*$ this decorrelation time diverges.

Another measure of configurational decorrelation is given by the following site-site autocorrelation function:

$$g(t) = \left\langle \frac{1}{N} \sum_{i=1}^N |r_i(t) - r_i(0)|^2 \right\rangle = 2\langle R_g^2 \rangle - \frac{2}{N} \left\langle \sum_{i=1}^N \mathbf{r}_i(0) \cdot \mathbf{r}_i(t) \right\rangle. \quad (34)$$

For the $N=4$ and 5 chains studied here the time evolution of this function mirrors that of the end-to-end vector correlation function, exhibiting a rapid rise at short times followed by an exponential-like approach to the asymptotic value of $2\langle R_g^2 \rangle$. The latter long-time behavior is approximately described by $g(t)/\langle R_g^2 \rangle \approx 2 - A \cos(\omega t) \exp(-t/\tau)$ where the oscillation frequency ω and “decay time” τ exhibit a similar L dependence as found above for the end-to-end vector correlations. Thus we again find that compared to the nonrotating chain, slow to moderate rotation speeds up configurational decorrelation while fast rotation dramatically slows this decorrelation process. The one notable difference in behavior between the Eqs. (33) and (34) correlation functions is that for the nonrotating chain (i.e., $L^*=0$) the Eq. (34) site-site correlation functions exhibit a distinct ripple or small amplitude oscillation that is damped out by time $\tau/2$. This oscillatory behavior is similar to, although nowhere near as dramatic as the oscillations observed by Deutsch in this correlation function for an isolated non-rotating Gaussian (i.e., non-self-interacting) chain with fixed bond lengths and conserved angular momentum [10]. Deutsch found that the addition of a repulsive site-site interaction completely eliminated these oscillations, resulting in a monotonic “decay” of this autocorrelation function. The ripple behavior that we observe for short repulsive chains decreases in magnitude with increasing chain length, becoming reduced to a minor oscillation in curvature for longer chains such as those studied by Deutsch.

VI. DISCUSSION

The static and dynamic properties of an isolated polymer chain differ from those of a chain in thermal and mechanical contact with a many-body reservoir. The isolated chain is subject to the conservation of total energy, linear momentum, and angular momentum and can be treated as a classical dynamical system. For a polymer model that assumes fixed bond lengths (as studied here), the three-bead chain is an “integrable” system and thus exhibits regular dynamics. For a chain consisting of four or more beads, the system is non-integrable and thus we expect chaotic dynamics. Many body systems with an underlying chaotic dynamics are the usual

subject of statistical mechanics and here we have treated the isolated chain using the microcanonical ensemble modified to include the conservation of both linear and angular momentum. One of the working hypotheses of statistical mechanics is that phase-space (or ensemble) averages should be equal to time averages. Here we have directly tested this ergodic hypothesis by comparing phase space averages for configurational and energetic properties of short chains, obtained from the exact microcanonical partition function, with the corresponding time averages obtained from MD simulations. For the $N=4$ and $N=5$ chains we have found these phase space and time averages to agree, independent of initial conditions for the time averages, providing strong support for the assumptions of ergodicity and chaotic dynamics for these systems.

The average conformation and dynamics of these polymer chains is strongly dependent on angular momentum. For small angular momentum (e.g., $L^* \leq 0.25L_{\max}^*$) there is only a small perturbation to the average chain structure, relative to the nonrotating chain, as seen in the insets to Figs. 2 and 3. Here the dynamics is certainly driven by bead-bead collisions. However, the reduction in the end-to-end vector and site-site decorrelation times, even for slow chain rotation, suggests an additional contribution to the dynamics. This speedup of the dynamics is most likely due to single-bead collisions with the centrifugal barrier, which will occur for certain chain orientations. For large angular momentum, the chain is strongly distorted into a linear conformation, such that bead-bead collisions are no longer possible. In this situation the chain dynamics undergoes a dramatic slowdown, as seen in the steep rise in the end-to-end vector decorrelation time (shown in the Fig. 6 insets). This slowdown is consistent with the lower effective temperatures associated with the smaller vibrational kinetic energies. Even for fast chain rotation the system still appears to be ergodic with the dynamics completely driven by single-bead collisions with the centrifugal barrier. In the case of $N=4$, the largest values of L studied by MD simulations required very long simulation times to achieve time averages that were independent of initial conditions. The $N=4$ chain has three degrees of freedom ($f=3$), which is just above the Kolmogorov-Arnold-Moser (KAM) limit of $f=2$ for which a Hamiltonian system will be localized in isolated regions of phase space and thus be non-ergodic [21,22]. For $f \geq 3$, phase space will be connected by Arnold diffusion, however, near the KAM limit this process may be slow [23,24]. This may also account for the anomalously slow dynamics of the nonrotating $N=4$ chain. For $L=0$, the $N=4$ chain has larger end-to-end vector and site-site decorrelation times than the $N=5$ chain with the same energy per bead E/N or the same energy per degree of freedom E/f . This result is counter to the general expectation that these decorrelation times should increase with increasing chain length (which is in fact what we observe for longer chains [34]).

One would anticipate that the dynamics of the type of model system studied here will be slowed down by the introduction of an attractive site-site potential or by the addition of chain stiffness. One way to include chain stiffness would be to consider cases where $b > \sigma$, which is a particularly simple way to increase the persistence length of the

chain [3]. While a system with attractive interactions is likely to become nonergodic at a low enough energy or temperature (as discussed in the Introduction), it is not immediately clear how chain stiffness will affect the ergodicity of this model system. We plan to study both of these effects in future work.

One approach for studying systems with slow dynamics is to use Monte Carlo (MC) rather than MD simulation methods. The wide variety of allowed particle "moves" in an MC simulation (which can include nonphysical moves) can allow a system to escape from local potential energy minima that might tend to trap an MD trajectory. To study the isolated chain system via MC simulation, one can make use of the canonical ensemble discussed in Sec. III B. Thus one carries out a simulation at fixed temperature T and angular momentum \mathbf{L} and then uses Eq. (11) to relate the results to the corresponding microcanonical fixed energy E . In order to properly account for both the conservation of angular momentum and fixed bond-lengths one carries out a modified Metropolis sampling in the MC simulation in which the probability of a state is taken to be proportional to $\exp(-U_L/k_B T) (\det \mathbf{H}_N / \det \mathbf{I}_0)^{1/2}$ [9,18,36]. Such an approach has been used to study Lennard-Jones atomic clusters and may prove useful for further study of an isolated chain with attractive site-site potentials. We note that using a fixed temperature MD algorithm to study a system with conserved angular momentum is complicated by the fact that the standard MD thermostats are nonergodic for systems with multiple conserved dynamical quantities [17]. Thus a chain of thermostats is required to properly deal with the multiple constraints.

ACKNOWLEDGMENTS

This project was supported in part by the Donors of the American Chemical Society Petroleum Research Fund [Grants No. 364559-GB7 (J.L.S) and 41836-GB7 (M.P.T)]. Additional funding was provided to M.P.T by Hiram College and to J.L.S by the National Science Foundation (Grant No. DMR-0103704).

APPENDIX A: EXPLICIT REMOVAL OF MOMENTUM DEGREES OF FREEDOM IN CONSTRAINED SYSTEMS

The classical phase space of an N particle system consists of the set of $6N$ Cartesian position and momentum variables which can be represented by the two $3N$ dimensional column vectors $\mathbf{r}^T = (\mathbf{r}_1, \dots, \mathbf{r}_N)$ and $\mathbf{p}^T = (\mathbf{p}_1, \dots, \mathbf{p}_N)$. (The superscript T indicates the transpose of a vector or matrix.) If the Cartesian coordinate variables are subject to ℓ holonomic constraints, one typically makes a canonical transformation to a set of generalized coordinates $\{\mathbf{Q}, \mathbf{P}\}$ consisting of $3N - \ell$ "soft" position variables \mathbf{Q}_a and ℓ "hard" (i.e., constrained) position variables \mathbf{Q}_b [17,21,33]. The generalized momenta, conjugate to these position coordinates, are given (in matrix notation) by $\mathbf{P} = m\mathbf{G}\dot{\mathbf{Q}}$ where m is the particle mass and $\mathbf{G} = \mathbf{J}^T \mathbf{J}$ is the metric tensor associated with the coordinate transformation $\mathbf{r} = \mathbf{J}\mathbf{Q}$. In block matrix form we have

$$\begin{pmatrix} \mathbf{P}_a \\ \mathbf{P}_b \end{pmatrix} = m \begin{pmatrix} \mathbf{G}_a & \mathbf{G}_{ab} \\ \mathbf{G}_{ba} & \mathbf{G}_b \end{pmatrix} \begin{pmatrix} \dot{\mathbf{Q}}_a \\ \dot{\mathbf{Q}}_b \end{pmatrix}, \quad (\text{A1})$$

where \mathbf{G}_a and \mathbf{G}_b are square matrices of size $(3N - \ell)$ and ℓ , respectively. The Hamiltonian of the system is given by

$$K + U = \frac{m}{2} \dot{\mathbf{r}}^T \dot{\mathbf{r}} + U(\mathbf{r}) = \frac{1}{2m} \mathbf{P}^T \mathbf{G}^{-1} \mathbf{P} + U(\mathbf{Q}_a, \mathbf{Q}_b) \quad (\text{A2})$$

which, given the constraints on the hard variables $\mathbf{Q}_b = \mathbf{q}_b$ and $\dot{\mathbf{Q}}_b = 0$ (where the vector \mathbf{q}_b specifies the fixed values of the \mathbf{Q}_b variables), reduces to

$$K_a + U_a = \frac{1}{2m} \mathbf{P}_a^T \mathbf{G}_a^{-1} \mathbf{P}_a + U(\mathbf{Q}_a, \mathbf{q}_b). \quad (\text{A3})$$

Thus the Hamiltonian only depends on the soft variables $\{\mathbf{Q}_a, \mathbf{P}_a\}$ and one works within this reduced $6N - 2\ell$ dimensional phase space [17,33,37–40]. The microcanonical phase-space integral of the constrained system is given by

$$\omega(E) = \int d\mathbf{Q}_a \int d\mathbf{P}_a \delta(E - U_a - K_a). \quad (\text{A4})$$

Evaluation of the above momentum integral results in a conformation dependent factor of $\sqrt{\det(\mathbf{G}_a)}$ which has been much discussed in the literature [37–45].

In some situations it may be desirable to start with the full $\{\mathbf{Q}, \mathbf{P}\}$ phase space integral and remove the constrained $\{\mathbf{Q}_b, \mathbf{P}_b\}$ subspaces more explicitly. Formal removal of the ℓ hard position variables is readily accomplished using the delta function $\delta^{(\ell)}(\mathbf{Q}_b - \mathbf{q}_b)$, however, proper removal of the corresponding momentum variables is not so straightforward. In particular, since \mathbf{P}_b is comprised of linear combinations of both hard and soft velocity variables [see Eq. (A1)], neither $\delta^{(\ell)}(\dot{\mathbf{Q}}_b)$ or $\delta^{(\ell)}(\mathbf{P}_b)$ will properly impose the velocity constraints in the phase space integral. To determine a procedure for explicitly removing the constrained momentum degrees of freedom it is useful to consider the inverse of Eq. (A1): $\dot{\mathbf{Q}} = \mathbf{H}\mathbf{P}/m$ or, in block form,

$$\begin{pmatrix} \dot{\mathbf{Q}}_a \\ \dot{\mathbf{Q}}_b \end{pmatrix} = \frac{1}{m} \begin{pmatrix} \mathbf{H}_a & \mathbf{H}_{ab} \\ \mathbf{H}_{ba} & \mathbf{H}_b \end{pmatrix} \begin{pmatrix} \mathbf{P}_a \\ \mathbf{P}_b \end{pmatrix}, \quad (\text{A5})$$

where $\mathbf{H} = \mathbf{G}^{-1}$. The velocities of the hard variables are given by $\dot{\mathbf{Q}}_b = (\mathbf{H}_{ba}\mathbf{P}_a + \mathbf{H}_b\mathbf{P}_b)/m$ which suggests that we examine the delta function $\delta^{(\ell)}(m\mathbf{H}_b^{-1}\dot{\mathbf{Q}}_b) = \delta^{(\ell)}(\mathbf{P}_b + \mathbf{H}_b^{-1}\mathbf{H}_{ba}\mathbf{P}_a)$ to accomplish the proper removal of the \mathbf{P}_b subspace. Note that this delta function strictly enforces the velocity constraints since each argument is simply a linear combination of the individual constraints. Inserting both this velocity-constraint and the position-constraint delta functions into the full microcanonical phase-space integral gives

$$\begin{aligned}
\omega(E) &= \int d\mathbf{Q}_a d\mathbf{Q}_b \delta^{(\ell)}(\mathbf{Q}_b - \mathbf{q}_b) \int d\mathbf{P}_a d\mathbf{P}_b \delta^{(\ell)}(\mathbf{P}_b \\
&\quad + \mathbf{H}_b^{-1} \mathbf{H}_{ba} \mathbf{P}_a) \times \delta\left(E - U(\mathbf{Q}_a, \mathbf{Q}_b) - \frac{1}{2m} \mathbf{P}^T \mathbf{H} \mathbf{P}\right) \\
&= \int d\mathbf{Q}_a \int d\mathbf{P}_a \delta\left(E - U(\mathbf{Q}_a, \mathbf{q}_b) \right. \\
&\quad \left. - \frac{1}{2m} \mathbf{P}_a^T (\mathbf{H}_a - \mathbf{H}_{ab} \mathbf{H}_b^{-1} \mathbf{H}_{ba}) \mathbf{P}_a\right) \\
&= \int d\mathbf{Q}_a \int d\mathbf{P}_a \delta\left(E - U(\mathbf{Q}_a, \mathbf{q}_b) - \frac{1}{2m} \mathbf{P}_a^T \mathbf{G}_a^{-1} \mathbf{P}_a\right),
\end{aligned} \tag{A6}$$

where, in writing the final expression, we have made use of the well known partitioning rules for block matrices [46]. The final expression of Eq. (A6) is identical to Eq. (A4) thus demonstrating that proper explicit removal of the momentum degrees of freedom associated with the constrained variables \mathbf{Q}_b is provided by the delta function $\delta^{(\ell)}(\mathbf{P}_b + \mathbf{H}_b^{-1} \mathbf{H}_{ba} \mathbf{P}_a)$.

Finally, we note that the above procedure for proper explicit removal of constrained variables can be expressed in the original $\{\mathbf{r}, \mathbf{p}\}$ Cartesian coordinates. Given that the constrained position variables can be written in the form $\mathbf{Q}_b = \mathbf{C}_b^T \mathbf{r}$, the position and momentum constraints are given by $\delta^{(\ell)}(\mathbf{C}_b^T \mathbf{r} - \mathbf{q}_b)$ and $\delta^{(\ell)}[(\mathbf{C}_b^T \mathbf{C}_b)^{-1} \mathbf{C}_b^T \mathbf{p}]$, respectively, where we have used $\mathbf{p} = m\dot{\mathbf{r}}$. These are the delta functions that appear in Eq. (5). See Ref. [25] for a recent alternate derivation of this result.

APPENDIX B: EVALUATION OF THE MOMENTUM INTEGRALS WITH BOND CONSTRAINTS

In performing the momentum integrations in Eq. (5) we have closely followed the approach of Calvo and Labastie (CL), Ref. [9], and we adapt their notation here. We first rewrite the bond velocity constraints as an $N-1$ dimensional delta function $\delta^{(N-1)}(\mathbf{H}_N^{-1} \mathbf{C}_N^T \mathbf{p})$ where, as in Appendix A, $\mathbf{p}^T = (\mathbf{p}_1, \dots, \mathbf{p}_N)$ is a $3N$ vector,

$$\mathbf{C}_N(\mathbf{r}) = \begin{pmatrix} -\hat{\mathbf{r}}_{1,2} & 0 & 0 & \dots \\ \hat{\mathbf{r}}_{1,2} & -\hat{\mathbf{r}}_{2,3} & 0 & \dots \\ 0 & \hat{\mathbf{r}}_{2,3} & -\hat{\mathbf{r}}_{3,4} & \\ 0 & 0 & \hat{\mathbf{r}}_{3,4} & \ddots \\ \vdots & \vdots & & \ddots & -\hat{\mathbf{r}}_{N-1,N} \\ & & & & \hat{\mathbf{r}}_{N-1,N} \end{pmatrix} \tag{B1}$$

is a $3N \times (N-1)$ matrix, $\mathbf{H}_N = \mathbf{C}_N^T \mathbf{C}_N$ is an $(N-1) \times (N-1)$ square matrix, and $\mathbf{r}^T = (\mathbf{r}_1, \dots, \mathbf{r}_N)$ is a $3N$ vector.

We now combine the 6 vector $\mathbf{b} = (\mathbf{L}, \mathbf{P}_{\text{tot}})$ with the $N-1$ dimensional null vector to form the $6+(N-1)$ vector $\mathbf{d}^T = (\mathbf{L}, \mathbf{P}_{\text{tot}}, 0, \dots, 0)$. Similarly, we combine the matrix $(\mathbf{H}_N^{-1} \mathbf{C}_N^T)^T$ with CL's $3N \times 6$ matrix $\mathbf{B}(\mathbf{r})$ to form a $3N \times (6+N-1)$ dimensional matrix $\mathbf{D}(\mathbf{r}) = [\mathbf{B}, (\mathbf{H}_N^{-1} \mathbf{C}_N^T)^T]$, where

$$\mathbf{B}(\mathbf{r}) = \begin{pmatrix} \mathbf{J}_1 & \mathbf{I} \\ \vdots & \vdots \\ \mathbf{J}_N & \mathbf{I} \end{pmatrix}, \tag{B2}$$

where \mathbf{I} is the 3×3 identity matrix and

$$\mathbf{J}_i = \begin{pmatrix} 0 & z_i & -y_i \\ -z_i & 0 & x_i \\ y_i & -x_i & 0 \end{pmatrix} \tag{B3}$$

with $(x_i, y_i, z_i) = \mathbf{r}_i^T$. Finally, defining the $3N \times 3N$ diagonal matrix \mathbf{A} , with elements $A_{i,j} = \delta_{ij}/2m$ and the scalar $a = E - V(\mathbf{r})$, the $3N$ -dimensional momentum integral in Eq. (5) can be written as

$$\Lambda_r(\mathbf{A}, \mathbf{D}, a, \mathbf{d}) = \int d^{3N} \mathbf{p} \delta(\mathbf{p}^T \mathbf{A} \mathbf{p} - a) \delta^{(6+N-1)}(\mathbf{D}^T \mathbf{p} - \mathbf{d}), \tag{B4}$$

where the first (1 dim) delta function gives the constraint on total energy and the second ($6+N-1$ dim) delta function combines the six linear and angular momentum constraints with the $N-1$ bond velocity constraints. CL have provided the general solution to integrals of the form of Eq. (B4), and thus we have

$$\Lambda_r(\mathbf{A}, \mathbf{D}, a, \mathbf{d}) = \frac{\pi^{f/2}}{\Gamma(f/2)} \frac{[a - \mathbf{d}^T (\mathbf{D}^T \mathbf{A}^{-1} \mathbf{D})^{-1} \mathbf{d}]^{f/2-1}}{\sqrt{\det \mathbf{A} \det (\mathbf{D}^T \mathbf{A}^{-1} \mathbf{D})}}, \tag{B5}$$

where $f = 3N - (6+N-1) = 2N-5$. Direct calculation yields

$$\mathbf{D}^T \mathbf{A}^{-1} \mathbf{D} = \left(\begin{array}{c|c} \mathbf{B}^T \mathbf{A}^{-1} \mathbf{B} & 0 \\ \hline 0 & (\mathbf{H}_N^{-1} \mathbf{C}_N^T) \mathbf{A}^{-1} (\mathbf{H}_N^{-1} \mathbf{C}_N^T)^T \end{array} \right), \tag{B6}$$

where the block diagonal form indicates that the linear and angular momentum constraints are uncoupled from the bond velocity constraints. (We note that this block diagonal form is only achieved if all sites have the same mass.) Noting that $\mathbf{C}_N^T \mathbf{A}^{-1} \mathbf{C}_N = 2m \mathbf{H}_N$, it is seen that the lower right block of Eq. (B6) simplifies to $2m(\mathbf{H}_N^{-1})^T$. The required determinant of the Eq. (B6) matrix factors as

$$\begin{aligned}
\det(\mathbf{D}^T \mathbf{A}^{-1} \mathbf{D}) &= \det(\mathbf{B}^T \mathbf{A}^{-1} \mathbf{B}) \det(2m \mathbf{H}_N^{-1}) \\
&= 2^6 (Nm)^3 \det(\mathbf{I}_o) \frac{(2m)^{N-1}}{\det(\mathbf{H}_N)},
\end{aligned} \tag{B7}$$

where \mathbf{I}_o is the moment of inertia tensor about the chain's center of mass. The \mathbf{H}_N matrix has the following tridiagonal form:

$$\mathbf{H}_N = \begin{pmatrix} 2 & -\hat{\mathbf{r}}_{12} \cdot \hat{\mathbf{r}}_{23} & 0 & 0 & \cdots & \\ -\hat{\mathbf{r}}_{12} \cdot \hat{\mathbf{r}}_{23} & 2 & -\hat{\mathbf{r}}_{23} \cdot \hat{\mathbf{r}}_{34} & 0 & \cdots & \\ 0 & -\hat{\mathbf{r}}_{23} \cdot \hat{\mathbf{r}}_{34} & 2 & \ddots & & \\ 0 & 0 & \ddots & \ddots & & \\ \vdots & \vdots & & & & \\ & & & & 2 & -\hat{\mathbf{r}}_{N-2,N-1} \cdot \hat{\mathbf{r}}_{N-1,N} \\ -\hat{\mathbf{r}}_{N-2,N-1} \cdot \hat{\mathbf{r}}_{N-1,N} & & & & & 2 \end{pmatrix} \quad (\text{B8})$$

with determinant given by the following recursive relations provided by Fixman [39],

$$\begin{aligned} \det \mathbf{H}_N &= 2 \det \mathbf{H}_{N-1} - (\hat{\mathbf{r}}_{N-2,N-1} \cdot \hat{\mathbf{r}}_{N-1,N})^2 \det \mathbf{H}_{N-2}, \\ \det \mathbf{H}_2 &= 2, \\ \det \mathbf{H}_1 &= 1. \end{aligned} \quad (\text{B9})$$

(The appearance of $\det \mathbf{H}_N$ in the solution to the momentum integral for a chain with bond-length constraints was first found by Kramers [37] and, as noted in Appendix A, has been much discussed in the literature.)

The required inverse of $\mathbf{D}^T \mathbf{A}^{-1} \mathbf{D}$ can be written as

$$(\mathbf{D}^T \mathbf{A}^{-1} \mathbf{D})^{-1} = \left(\begin{array}{c|c} (\mathbf{B}^T \mathbf{A}^{-1} \mathbf{B})^{-1} & 0 \\ \hline 0 & \mathbf{H}_N/2m \end{array} \right) \quad (\text{B10})$$

and thus, recalling that $\mathbf{d}^T = (\mathbf{L}, \mathbf{P}_{\text{tot}}, 0, \dots, 0)$, we have

$$\begin{aligned} \mathbf{d}^T (\mathbf{D}^T \mathbf{A}^{-1} \mathbf{D})^{-1} \mathbf{d} &= \mathbf{b}^T (\mathbf{B}^T \mathbf{A}^{-1} \mathbf{B})^{-1} \mathbf{b} \\ &= (\mathbf{L} - \mathbf{L}_o)^T \frac{I_o^{-1}}{2} (\mathbf{L} - \mathbf{L}_o) + \frac{\mathbf{P}_{\text{tot}}^2}{2m}, \end{aligned} \quad (\text{B11})$$

where the final result is CL's Eq. (10) and $\mathbf{L}_o = \mathbf{r}_o \times \mathbf{P}_{\text{tot}}$, where \mathbf{r}_o is the position of the center of mass for configuration \mathbf{r} and \mathbf{P}_{tot} is the total linear momentum. In the text we consider $\mathbf{P}_{\text{tot}} = 0$, which is equivalent to working in the chain center-of-mass coordinate system and for which case \mathbf{L}_o also vanishes, which leads to Eq. (6).

APPENDIX C: 3-MER CHAIN EQUATIONS OF MOTION

The dynamics of the 3-mer chain can be described in terms of the internal motion of the interaction sites relative to the chain CM and the rotational motion of the body frame with respect to a set of fixed space axes. The internal motion, which is confined to the body frame xz plane, is completely described by the time evolution of the distance r_{13} and the body frame motion can be described by the time variation of a set of Euler angles that specify the orientation of the body frame in space [21,47]. If we take the fixed space z axis to lie along the \mathbf{L} vector, two of these Euler angles are simply related to the angles θ and φ defined in Eq. (20). The equation of motion for r_{13} can be obtained directly from the Eq. (9) energy conservation expression and is given by

$$\begin{aligned} (\dot{r}_{13})^2 &= \frac{6}{m} \left(\frac{4b^2 - r_{13}^2}{6b^2 - r_{13}^2} \right) [E - K_{\text{rot}}(r_{13}, \theta, \varphi) - u(r_{13})], \\ r_{\min} &< r_{13} < r_{\max}, \end{aligned} \quad (\text{C1})$$

where K_{rot} is given by Eq. (24) and r_{\min} and r_{\max} are set by the roots of $E = K_{\text{rot}}(r_{13}) - u(r_{13})$ such that $r_{\max} < 2b$. Equation (C1) shows that the internal motion of the chain is coupled to the orientation of the body frame through the angles θ and φ . The equations of motion for these angles can be constructed using the following set of Euler equations:

$$\frac{d}{dt} (I_{\alpha\alpha} \Omega_\alpha) = (I_{\beta\beta} - I_{\gamma\gamma}) \Omega_\beta \Omega_\gamma, \quad (\text{C2})$$

where Ω_α is the alpha component of the chain angular velocity in the body frame such that $L_\alpha = I_{\alpha\alpha} \Omega_\alpha$ where the Cartesian components of $\mathbf{L}(\theta, \varphi)$ in the body frame are given by Eq. (20) and $\{\alpha, \beta, \gamma\} \rightarrow \{x, y, z\}$ with cyclic permutations. Equation (C2) applies to the force free motion of a nonrigid body whose principle axes are independent of the internal motion of the body. Combining Eqs. (C2) and (20) yields

$$\dot{\theta} = -\frac{L}{2} \left(\frac{I_{yy} - I_{xx}}{I_{yy} I_{xx}} \right) \sin \theta \sin 2\varphi \quad (\text{C3})$$

and

$$\dot{\varphi} = -L \cos \theta \left\{ \frac{I_{yy} - I_{xx}}{I_{yy} I_{xx}} \sin^2 \varphi + \frac{I_{xx} - I_{zz}}{I_{xx} I_{zz}} \right\}, \quad (\text{C4})$$

where explicit expressions for the principle moments of inertia in terms of r_{13} have been given previously and we note that $I_{yy} > I_{xx} > I_{zz}$ for $r_{13} < b$ and $I_{yy} > I_{zz} > I_{xx}$ for $r_{13} > b$. Equations (C3) and (C4) demonstrate that for principle axis rotation (i.e., $\{\theta, \varphi\} = \{\pi/2, 0\}$, $\{\pi/2, \pi/2\}$, $\{0, \varphi\}$), the orientation of the \mathbf{L} vector remains fixed within the body frame. For nonprinciple axis rotation the motion is complex, depending on the initial \mathbf{L} vector, the initial value of r_{13} and the initial sign of \dot{r}_{13} . We have solved the above set of coupled equations for $r_{13}(t)$, $\theta(t)$, and $\varphi(t)$ using a fourth-order Runge-Kutta algorithm and find good agreement with our 3-mer chain MD simulation results. To study the time evolution of the absolute orientation of the chain in space requires an additional equation of motion for the third Euler angle [47]. While construction of this equation is straightforward, we have not pursued it here as our interest is in the internal motion of the chain.

- [1] P.-G. de Gennes, *Scaling Concepts in Polymer Physics* (Cornell University Press, Ithaca, 1979).
- [2] M. Doi and S. F. Edwards, *The Theory of Polymer Dynamics* (Clarendon Press, Oxford, 1986).
- [3] A. Yu. Grosberg and A. R. Khokhlov, *Statistical Physics of Macromolecules* (AIP, New York, 1994).
- [4] P. Thaddeus, M. C. McCarthy, M. J. Travers, C. A. Gottlieb, and W. Chen, *Faraday Discuss.* **109**, 121 (1998).
- [5] M. B. Bell, P. A. Feldman, J. K. G. Watson, M. C. McCarthy, M. J. Travers, C. A. Gottlieb, and P. Thaddeus, *Astrophys. J.* **518**, 740 (1999).
- [6] Ph. Dugourd, R. R. Hudgins, D. E. Clemmer, and M. F. Jarrold, *Rev. Sci. Instrum.* **68**, 1122 (1997).
- [7] M. F. Jarrold, *Phys. Chem. Chem. Phys.* **9**, 1659 (2007).
- [8] R. S. Dumont, *J. Chem. Phys.* **95**, 9172 (1991).
- [9] F. Calvo and P. Labastie, *Eur. Phys. J. D* **3**, 229 (1998).
- [10] J. M. Deutsch, *Phys. Rev. Lett.* **99**, 238301 (2007).
- [11] J. M. Deutsch, *Phys. Rev. E* **77**, 051804 (2008).
- [12] L. E. Reichl, *A Modern Course in Statistical Physics* (University of Texas Press, Austin, 1980).
- [13] Ya. G. Sinai, *Russ. Math. Surveys* **25**, 137 (1970).
- [14] Ya. G. Sinai and N. I. Chernov, *Russ. Math. Surveys* **42**, 181 (1987).
- [15] L. Bunimovich, C. Liverani, A. Pellegrinotti, and Y. Suhov, *Commun. Math. Phys.* **146**, 357 (1992).
- [16] J. R. Dorfman, *An Introduction to Chaos in Nonequilibrium Statistical Mechanics* (Cambridge University Press, Cambridge, UK, 1999).
- [17] D. Frenkel and B. Smit, *Understanding Molecular Simulation* (Academic Press, San Diego, 2002).
- [18] F. Calvo, J. Galindez, and F. X. Gadea, *J. Phys. Chem. A* **106**, 4145 (2002).
- [19] N. Sreenath, Y. G. Oh, P. S. Krishnaprasad, and J. E. Marsden, *Dyn. Stab. Syst.* **3**, 25 (1988).
- [20] Y. G. Oh, N. Sreenath, P. S. Krishnaprasad, and J. E. Marsden, *J. Dyn. Differ. Equ.* **1**, 269 (1989).
- [21] L. N. Hand and J. E. Finch, *Analytical Mechanics* (Cambridge University Press, Cambridge, UK, 1998).
- [22] A. J. Lichtenberg and M. A. Lieberman, *Regular and Chaotic Dynamics*, 2nd ed. (Springer, New York, 1992).
- [23] B. P. Wood, A. J. Lichtenberg, and M. A. Lieberman, *Physica D* **71**, 132 (1994).
- [24] P. M. Cincotta, *New Astron. Rev.* **46**, 13 (2002).
- [25] G. R. Kneller, *J. Chem. Phys.* **125**, 114107 (2006).
- [26] M. P. Taylor, *J. Chem. Phys.* **114**, 6472 (2001).
- [27] J. Jellinek and D. H. Li, *Phys. Rev. Lett.* **62**, 241 (1989).
- [28] E. M. Pearson, T. Halicioglu, and W. A. Tiller, *Phys. Rev. A* **32**, 3030 (1985).
- [29] T. Cagin and J. R. Ray, *Phys. Rev. A* **37**, 247 (1988).
- [30] M. P. Taylor, *J. Chem. Phys.* **118**, 883 (2003).
- [31] J. P. Ryckaert, G. Ciccotti, and H. J. C. Berendsen, *J. Comput. Phys.* **23**, 327 (1977).
- [32] H. C. Andersen, *J. Comput. Phys.* **52**, 24 (1983).
- [33] M. P. Allen and D. J. Tildesley, *Computer Simulation of Liquids* (Oxford University Press, Oxford, UK, 1987).
- [34] K. Isik, M.S. thesis, University of Akron, Akron, OH, 2004.
- [35] J. P. Hansen and I. R. McDonald, *Theory of Simple Liquids* (Academic, London, 1986), Chap. 7.
- [36] M. Fixman, *J. Chem. Phys.* **69**, 1527 (1978); **69**, 1538 (1978).
- [37] H. A. Kramers, *J. Chem. Phys.* **14**, 415 (1946).
- [38] O. Hassager, *J. Chem. Phys.* **60**, 2111 (1974).
- [39] M. Fixman, *Proc. Natl. Acad. Sci. U.S.A.* **71**, 3050 (1974).
- [40] N. Go and H. A. Scheraga, *Macromolecules* **9**, 535 (1976).
- [41] M. Gottlieb and R. B. Bird, *J. Chem. Phys.* **65**, 2467 (1976).
- [42] E. Helfand, *J. Chem. Phys.* **71**, 5000 (1979).
- [43] K. G. Honnell, C. K. Hall, and R. Dickman, *J. Chem. Phys.* **87**, 664 (1987).
- [44] H. M. Adland and A. Mikkelsen, *J. Chem. Phys.* **120**, 9848 (2004).
- [45] A. Patriciu, G. S. Chirikjian, and R. V. Pappu, *J. Chem. Phys.* **121**, 12708 (2004).
- [46] W. H. Beyer, *CRC Standard Mathematical Tables*, 25th ed. (CRC, Boca Raton, 1979), p. 31.
- [47] L. D. Landau and E. M. Lifshitz, *Mechanics* (Pergamon, Oxford, 1969), Secs. 35–37.